Aridity synthesis for 8 selected key regions of the global climate system during the last 60 000 years

Florian Fuhrmann[1], Benedikt Diensberg[1], Xun Gong[2], Gerrit Lohmann[2], Frank Sirocko[1]

[1]Department for Geoscience, Johannes-Gutenberg-Universität, Mainz, 55099, Germany
[2]Alfred Wegener Institute for Polar and Marine Research, Bremerhaven, Germany

Correspondence to: Florian Fuhrmann, (flfuhrma@uni-mainz.de)

Supplements:

S1 Arabian Sea:

The Arabian Sea comprises the region from the Persian Gulf to the Indian Sea and is characterized by warm and high saline waters and fluvial input from the Indus River. High dust fluxes mainly from Arabian desert are preserved in the sediments. The high surface-water productivity from monsoonal inputs into the ocean and upwelling offshore west Pakistan lead to a stable oxygen minimum zone (OMZ) in water depths between 200 m and 1200 m. This OMZ results in excellent preservation conditions for dark, organic-carbon rich, laminated sediments during mild interstadials and in contrast to light colored, bioturbated sediments during stadials and especially Heinrich events (Schulz, et al., 1998). Arabian Sea and North Atlantic regions are closely coupled by atmospheric teleconnections (Burns et al., 2003; Deplazes et al., 2014; Leuschner and Sirocko, 2000, 2003; Schulz, et al., 1998; Sirocko et al., 1996a and others). There is evidence for a general relationship between these two regions on timescales of the last 110 000 years within low-latitude monsoonal variability and high northern latitude records of Greenland ice cores (Schulz, et al., 1998). The sediment cores SO130-289KL and SO90-136KL are from very close positions and show nearly the same pattern within Reflectance and Total Organic Carbon (TOC) content. Furthermore, they can be correlated one-to-one to the NGRIP ice core (North Greenland Ice Core Project Members et al., 2004) on every GI from 17 to 1 and the YD cold event. In Addition, the Heinrich events 6 to 1 (H6 - H1) appear in superposition (see Fig. S1). The speleothem growth in this region can be correlated to the Greenland ice cores as well (Burns et al., 2003). Speleothems from Oman and Socotra Cave in Yemen are very close to the Arabian Sea and hence used for this synthesis. The sediment core 70KL shows $CaCO_3$ content in percent as a dust indicator. High $CaCO_3$ values show low dust contents from Arabian Peninsula desert and vice versa – more dust accounts for lower $CaCO_3$ values due to higher dilution of the sediment because of increased sedimentation rates.

From 60 000 to 55 000 yr b2k no speleothem growth is apparent for the Arabian sea region while the dust values show a maximum. The Reflectance data simultaneously show very high values (according to bioturbation) indicating the extend of H6 to this region. The TOC content is on small values resulting from only slight upwelling and low bioproduction but still all

GIs are visible with less expression compared to the NGRIP ice core. The dust reconstruction from $CaCO_3$ content shows high amounts in dust values. A high aridity is reconstructed for this period.

From 55 000 to 41 800 yr b2k, the GIs 14 to 11 are visible in the TOC. High variations between stadial and interstadial times occur with the highest values of about 5% TOC during GI14 and 12. The lowest values go along with H5, but in general, stadials account for lower TOC values. In the time of 55 000 to 41 800 yr b2k, the mean TOC values were on the highest values for the last 60 000 years. Also, the Reflectance data show this pattern with clearly visible H5 and GI expression. Within the dust content, a minimum during this period is apparent (lowest values beside the Holocene) and speleothem growth occurred in the Socotra Cave during this early MIS3 time indicating high precipitation and strong monsoonal variability resulting in low aridity as visible in the aridity index (see Fig. S1e).

From 41 800 to 27 700 yr b2k the GIs 10 to 3 are present within Reflectance and TOC data and comparable to the NGRIP ice core. Intermediate TOC values and the large differences between interstadial and stadial, especially at H4 and H3 times, are remarkable. The dust content varies between high and medium values through this period with higher values around 35 000 yr b2k and lower values during GI5. This interstadial seems to be nearly as strong as GI12, which is known as one of the 'warmest interstadials' for several regions within TOC and Reflectance data. No speleothem growth is observed during the high glacial period. The aridity was high at the beginning of this phase. GI5 and the double GI3 and 4 appear to have had strong impact on the precipitation, so the aridity was lower during this time with an increase to stronger aridity afterwards.

Between 27 700 and 11 700 yr b2k are GI2 and 1 as well as H2 and H1 and the YD apparent. The TOC decreases from high values at the end of GI3 to very low ones during LGM and especially H1 and YD. The dust remains on intermediate to high values with dust pulses within H1 and H2. These events increased aridity to very high values but the aridity within the rest of this time phase was high nevertheless.

With the onset of the Holocene at 11 700 yr b2k, speleothem growth in Oman caves started. The dust values decrease to minimum during the Holocene climate optimum around 8 000 to 6 000 yr b2k. The Reflectance and TOC data increase drastically and show higher temperature as well during early Holocene, with a slight decrease towards present day. During early Holocene times the precipitation seems very strong with low aridity. Towards present day, the aridity increases strongly.

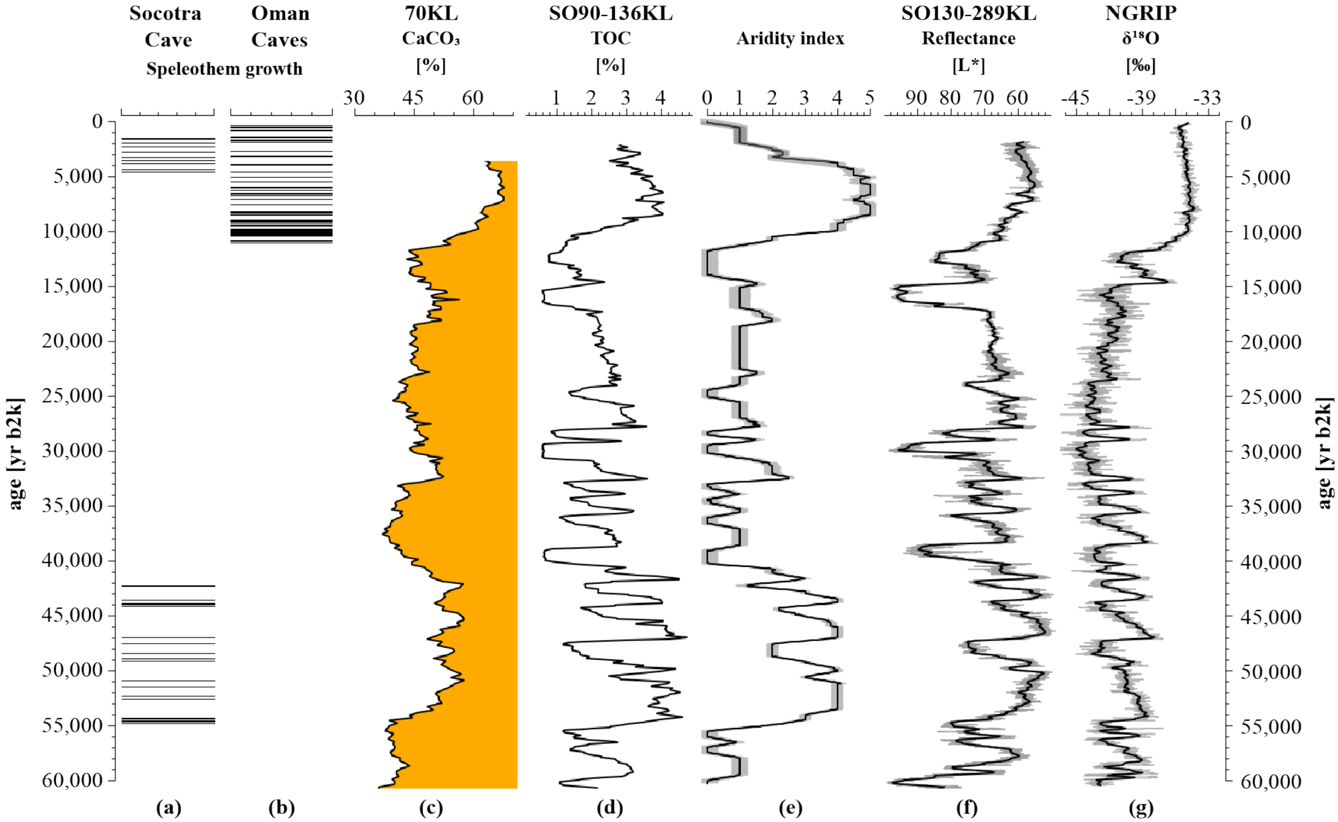

Figure S1: Arabian Sea climate over the last 60 000 years: **(a)** Socotra Cave and **(b)** Oman Caves (Burns et al., 2003; Fleitmann et al., 2007) show speleothem growth phases, which require mobile water from frequent precipitation; **(c)** 70KL $CaCO_3$ (Leuschner and Sirocko, 2003) indicates more arid conditions with lower values, higher values account for more humid conditions; **(d)** SO90-136KL (Schulz, et al., 1998) TOC content exhibits the GIs comparable to **(g)** in total by higher carbon values; **(e)** Aridity index for Central Europe as result from **(a-d),** for detailed information see method section; **(f)** SO130-289KL Reflectance data (Deplazes et al., 2014) resembling **(d)** and **(g); (g)** $\delta^{18}O$ data from NGRIP ice core (North Greenland Ice Core Project Members et al., 2004) in comparison.

S2 North-West Africa:

To understand the climate history of North-West Africa and the continental margin off West Africa is important for understanding changes in Sahara – Sahel aridification as induced by changes in Atlantic water sea surface temperatures (SST) or large scale mechanisms like for example AMOC, North Atlantic Oscillation (NAO), Inter Tropical Convergence Zone (ITCZ). Life in this region strongly depends on the availability of water. Nowadays, the mean annual temperature ranges between 12 and 15 °C and mean annual precipitation is about 468 mm/yr for Atlas Mountain ranges related to the Azores high position (Wassenburg et al., 2012). Sediment core GIK15627-3 from offshore Morocco reveals the time from 250 000 to 5 000 years b2k of paleovegetation for NW-Africa (Hooghiemstra et al., 1992). No long pollen time series are available from terrestrial archives right now, hence this record was chosen despite a relatively low sample resolution. Nearby speleothems are known from Atlas mountain range like Grotte Prison de Chien (Wassenburg et al., 2012) or Grotte de Piste (Wassenburg et al., 2016). GeoB9508-5, a sediment core from offshore Senegal, West Africa, (Collins et al., 2013; Mulitza et al., 2008) reveals strong Heinrich Stadials in dust content during times of reduced AMOC (Mulitza et al., 2008; see Fig. S2).

The timespan from 60 000 to 50 000 yr b2k comprises GI17 - 14. No Speleothem growth is apparent during the whole timespan. The amount of tree pollen decreases from values around 60 % to 0 % (53 000 yr b2k) and rises again during a wet period from 52 500 to 50 500 yr b2k. The dust content shows no major fluctuations during this phase and remains at its lowest levels until the beginning of the Holocene. Low dust values and varying tree pollen amounts, the aridity is on intermediate to lower values. Between 50 000 and 37 000 yr b2k with GI13 – 8, aridity is increased. A first speleothem age is known to be around 45 000 yr b2k, shortly after the end of H5. Tree pollen amount is constantly on lower values (~ 30 %) with a little decrease during H5. Dust values peak strongly during Heinrich Stadials 5 and 4 indicating intermediate to high aridity. From 37 000 to 27 000 yr b2k (GIs 7-3) NW-Africa underwent increasing aridity. Speleothem growth was only sporadic but comes along with higher tree pollen values for the same times. Tree pollen remain on lower values between 20 and 30 % with a small increase during the growth phases known from the speleothem. Dust content is on intermediate values with a small increase during H3 at the end of this period. The climate of this time phase appears cold and moderate arid. The onset to H2 marks the begin of the next period (27 000 to 14 800 yr b2k, GI2 within). Grotte Prison de Chien shows at least some dating indicating sporadic precipitation for this period. In general, tree pollen values decrease to very low values indicating even more arid conditions between 20 000 and 15 000 yr b2k (Hooghiemstra et al., 1992). The dust values are on a maximum during this phase in general but H2 and H1 are clearly identifiably within the record. With all that information combined, the period expresses the impact of the LGM period and shows arid and cold conditions. With the end of H1 and the onset of warming towards the Holocene, the amount of tree pollen increases again (14 800 yr b2k until present, GI1 and YD), while speleothems from North Morocco also show some growth phases. Gradually, less arid conditions show a climate amelioration until 8 500 yr b2k, the ‘African Humid Period’ (AHP) or EHTO (Early Holocene Temperature Optimum), where lots of age datings can be found indicating fast speleothem growth. Dust shows a small peak during YD cold event. However, the general strong decrease from the end of LGM until EHTO is evident. Little dust was mobile during this phase. In the last 4 000 years, dust values rise again, indicating an aridity increase for youngest times.

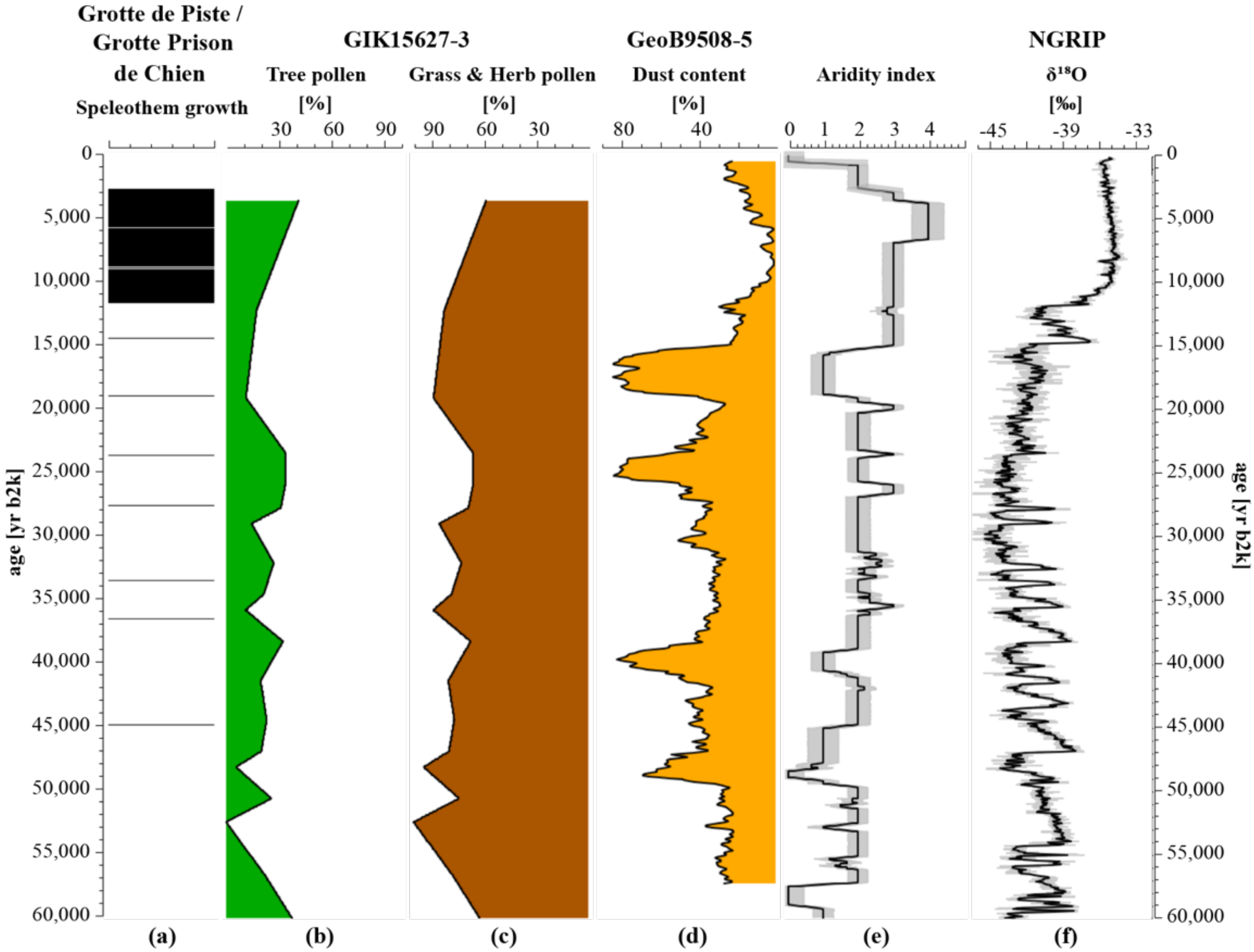

Figure S2: NW-Africa climate over the last 60 000 years: **(a)** Grotte Prison de Chien (Wassenburg et al., 2012) and Grotte de Prison (Wassenburg et al., 2016) show speleothem growth phases, which require mobile water from frequent precipitation; **(b, c)** GIK15627-3 marine core pollen data (Hooghiemstra et al., 1992) are divided into tree- and herb & grass pollen. While trees require more precipitation, grasses are dominant for more arid conditions; **(d)** GeoB9508-5 (Collins et al., 2013) indicates more arid conditions with higher values, lower values account for more humid conditions. HE are distinguishable by higher dust concentrations; **(e)** Aridity index for NW-Africa as result from **(a)-(d)**, for detailed information see method section; **(f)** $\delta^{18}O$ data from NGRIP ice core (North Greenland Ice Core Project Members et al., 2004) in comparison.

S3 China:

Most of the Asian continent is influenced by the East Asian Monsoon, which is the most important moisture source. Most of annual precipitation (~ 80 %) falls in summer season (e.g. Mingram et al., 2018; Wang et al., 2001) with mean annual precipitation about 1015 mm/yr at Hulu Cave and 715 mm/yr at Sihailongwan maar lake (Stebich et al., 2015). The mean annual temperature is about 2.9 °C (Schettler et al., 2006), varying from -18.1 °C for January and + 20.7 °C for July at Sihailongwan site and 15.4 °C at Hulu Cave (Wang et al., 2001).

Hulu Cave is one of the most popular east Asian monsoon records through the last glacial cycle. For this record, five speleothems from the cave were stacked together to compile a continuous record for the timespan of 11 000 – 75 000 yr b2k. The long-term trend follows summer insolation pattern, suggesting an increased summer continent-ocean temperature difference and so, enhanced summer monsoon (Wang et al., 2001). The Hulu record shows a link between East Asia Monsoon and North Atlantic climate by apparent GI-variations within the $\delta^{18}O$ record. The Sihailongwan maar lake (SHL) lies within the Long Gang Volcanic Field in NE-China. The SHL-core is continuously warved until 65 000 yr b2k, providing an excellent stratigraphy for climate reconstructions by not only paleovegetation. The tree pollen amount replicates the stadial / interstadial variations of the North Atlantic (see Fig. S3) as well as the total organic carbon. Stadials and especially Heinrich events are characterized by steppic plants like Artemisia. Interstadials in general show higher amounts of tree pollen (Mingram et al., 2018). However, the Holocene pollen data are not publically available for this paper but kept in mind for the discussion of this synthesis. The China Loess Plateau is well known for its loess paleosol sequences. Jingyuan and Weinan sections from Sun et al. (2010) and Lu et al. (2007) are established and show reliable indications for North Atlantic - China climate teleconnections with “loess interstadial / loess stadial” within the mean grainsize of the Jingyuan record.

The timespan from 60 000 yr b2k until 50 000 yr b2k (GI17 - GI13, early MIS3) is regarded as the most humid period of the record (Liu et al., 2010; Lu et al., 2007; Mingram et al., 2018). Speleothem growth is apparent and $\delta^{18}O$ values are on minimum (more negative equals higher temperatures, see (Liu et al., 2010; Wang et al., 2001)) during this period. The tree pollen show high values in order of 60 % with identifiable GI variability. Also, dust values from the Jingyuan loess section show small grainsizes according to a lower dust content. In result, the archives account for humid climate conditions through the early MIS3 phase. Within the period of 50 000 yr b2k to 34 000 yr b2k, GIs 12 to 5 are comprised. This phase also shows continuous speleothem growth with intermediate $\delta^{18}O$ values, GIs are easy to identify. Also, the tree pollen show medium contents with still relative high values during interstadials but lower compared to early MIS3 times. The dust content rises to intermediate values until 38 000 yr b2k indicating stronger winds and lower temperatures combined with a higher aridity. Towards the end of this phase, lower $\delta^{18}O$ values combined with the sharp GI-type increases in tree pollen and lower dust contents are visible, suggesting a phase of stagnation within the climate conditions.

From 34 000 yr b2k to 14 800 yr b2k (GIs 4-2) the climate is characterized by glacial conditions, especially during last glacial maximum and the Heinrich events 3 to 1. The growth rates of the Hulu Cave speleothems went down while the $\delta^{18}O$ values rise to their highest values of the record. Synchronously, the tree pollen decrease to about 20 % during LGM, with high contents of Artemisia especially during Heinrich events, the GIs during this phase are less expressive with general lower temperatures and shorter durations. Between 29 550 yr b2k and 18 250 yr b2k, the minimum of thermophilous plants and tree pollen is apparent (Mingram et al., 2018). The dust values are on a maximum during this time span. The large grainsize comes along with low temperatures and precipitation values. All that combined is clearly visible in the aridity index with a strong expressed

LGM. The deglaciation and the Holocene itself (14 800 yr b2k to present, GI1) can be characterized by the amelioration of the climate conditions, in China as well as on a global scale. The $\delta^{18}O$ values decrease while the growth rate increases. The tree pollen rise up to 80 % while synchronously the dust content lessens to the minimum of the record during the Holocene temperature optimum (6 000 yr b2k – 4 000 yr b2k). According to Stebich et al. (2015) the Sihailongwan Maar pollen indicate a maximum precipitation at 4 550 yr b2k (not included into Fig. S3). The aridity decreased during the Holocene transition to intermediate values, but a lack in data for the Holocene period makes it complicated to draw further estimates.

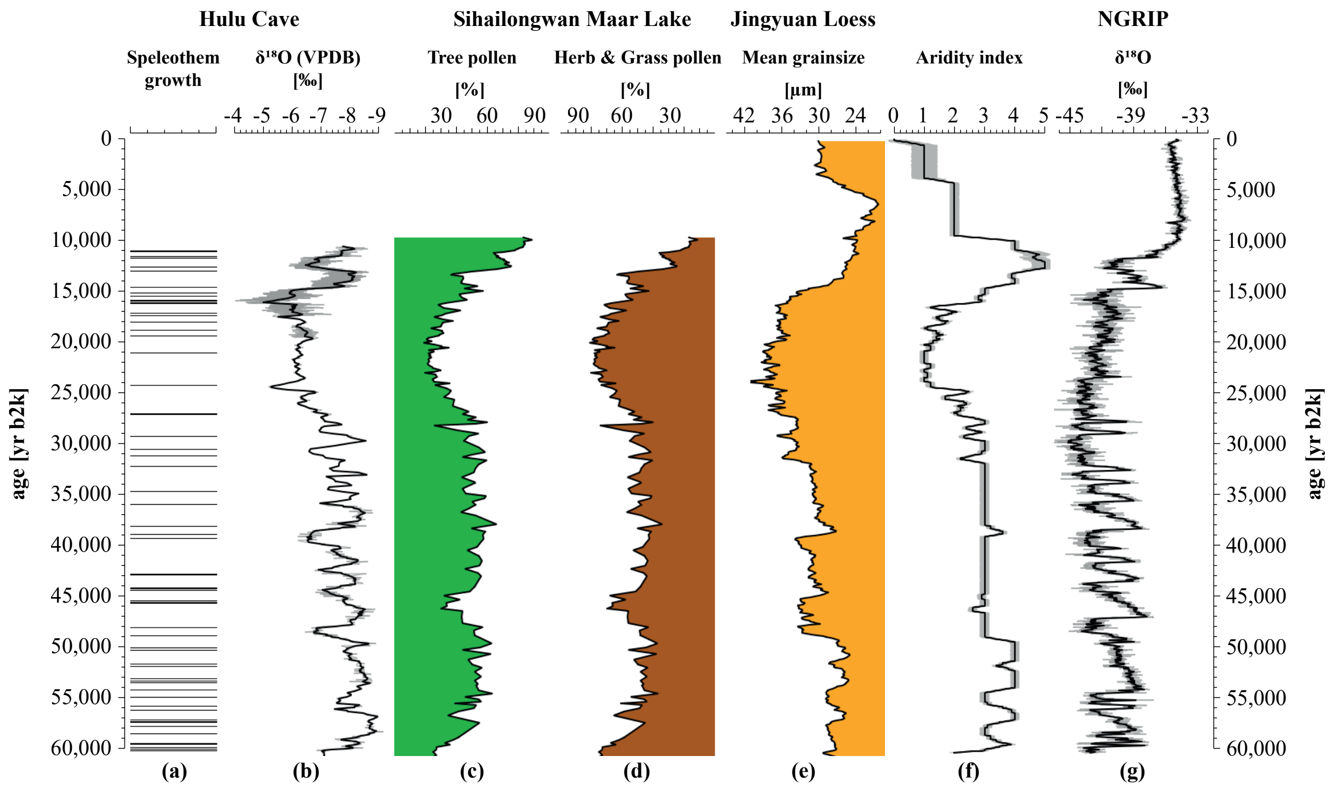

Figure S3: China climate over the last 60 000 years: **(a)** Hulu Cave (Liu et al., 2010; Wang et al., 2001) show speleothem growth phases, which require mobile water from frequent precipitation; **(b)** $\delta^{18}O$ data with apparent GIs comparable to **(g)**, more negative $\delta^{18}O$ values account for more humid conditions (Wang et al., 2001); **(c, d)** Sihailongwan Maar Lake pollen data (Mingram et al., 2018) are divided into tree- and herb & grass pollen. While trees require more precipitation, grasses are dominant for more arid conditions; **(e)** Jingyuan Loess mean grainsize (Sun et al., 2010) indicates more arid conditions with larger grains, smaller grains account for more humid conditions; **(f)** Aridity index for China as result from **(a-e)**, for detailed information see method section; **(g)** $\delta^{18}O$ data from NGRIP ice core (North Greenland Ice Core Project Members et al., 2004) in comparison.

S4 Southern Europe

Southern Europe is affected by the Atlantic Ocean water masses as well as from the Mediterranean Sea and so, influenced by changes in AMOC, NAO, ITCZ and other large-scale mechanisms. Nowadays, the mean annual temperature close to the

Villars Cave (in southern France) speleothem site is 12.1 °C and mean annual precipitation 1020 mm/yr, evenly spread through the whole year (Wainer et al., 2009). A sediment core of volcanic maar lake Lac du Bouchet (Lake Bouchet) shows pollen spectra until the end of the last interglacial (Reille and de Beaulieu, 1988, 1990). Although 'Nussloch paleosol loess sequence' (Antoine et al., 2001) is well established but publicly available data are not accessible. MD01-2443 marine sediment core (Hodell et al., 2013) is the closest dust archive with sufficient stratigraphy for Southern Europe. SST, L* (color reflectance) and $\delta^{18}O$ of the core show GIs (Hodell et al., 2013; Martrat et al., 2007). Well dated speleothem data are available for the Villars Cave, 200 km away from the Atlantic coast, with speleothem growth between 52 000 and 29 000 yr b2k and for the Holocene (see Fig. S4). The growth speed significantly slowed down between 42 000 and 29 000 yr b2k and finally stopped with the onset to LGM conditions. Also, a hiatus from 55 700 to 52 000 yr b2k is present within the record. GIs 14, 13, 12 and on minor extend GI11 are preserved as well as H5 (Genty et al., 2003; Wainer et al., 2009).

The timespan from 60 000 to 44 000 yr b2k incorporates GIs 17 to 12 within the records of this region. Speleothem growth in the Villars Cave is evident with a hiatus between 55 700 to 52 000 yr b2k. $\delta^{18}O$ values indicate warm and moist conditions with more negative values than during later phases of the record. The GIs 17, 16, 13 and 12 are identifiable within the data. According to Wainer et al. (2009) the temperature optimum of the recorded time phase was during early MIS3 at around 52 000 yr b2k. In contrast, the highest amount of tree pollen for this period (with about 50 %) falls within the hiatus of the speleothem but still indicating warm and wet early MIS3 conditions for this region. Also, dust content from marine sediment core MD01-2443 are on relatively low values with minor variations. Their lowest values until the Holocene were during the tree pollen maximum. Until the end of this time phase towards 45 000 yr b2k, conditions tend to get worse as indicated by rising dust content, decreasing amount of tree pollen, lower $\delta^{18}O$ values from Villars Cave and with H5 from the marine cores. The aridity is low during the early MIS3 phase and rises towards the end of the time phase.

The period from 44 000 to 30 000 yr b2k (GIs 11-5) shows general aridity (Reille and de Beaulieu, 1990). The speleothem $\delta^{18}O$ values are very low, only GI8 stands out a bit. The speleothem growth was significantly slower and stopped at the end of this time phase. The tree pollen show high variations and high absolute values, but high amount of steppe vegetation and a small remaining tree population complete the in general increased aridity for Southern Europe. The dust values replicate the interstadial / stadial changes with stronger impression on Heinrich events.

From 30 000 to 15 000 yr b2k (GIs 4-2) no speleothem growth is known from Villars Cave. The tree pollen show low values with a minimum around 25 000 yr b2k, were no tree pollen occur within the record. During LGM, grasses (60 to 100 %) replace the last Pinus woodland, which was still apparent at GI3 and 4. Dust values show arid conditions and low temperatures, Heinrich events are well expressed, apart from a low variability. Dust values are highest at the end of this period from 17 000 to 14 000 yr b2k during the same time, were Ruth et al. (2007) detected most eolian dust in NGRIP ice cores (cf. Fig. 2 and Fig. 6). The aridity was strongest during LGM especially during the end of this phase. With the onset towards the Holocene around 15 000 yr b2k, speleothem growth restarted in the Villars cave, the amount of tree pollen drastically increases and dust values decrease with a delay of approximately 4 000 years after YD cold event. The Altithermal is displayed by precipitation and temperature increase visible in the records. The aridity decreases with the onset of the Holocene and stays relatively constant on lower values throughout.

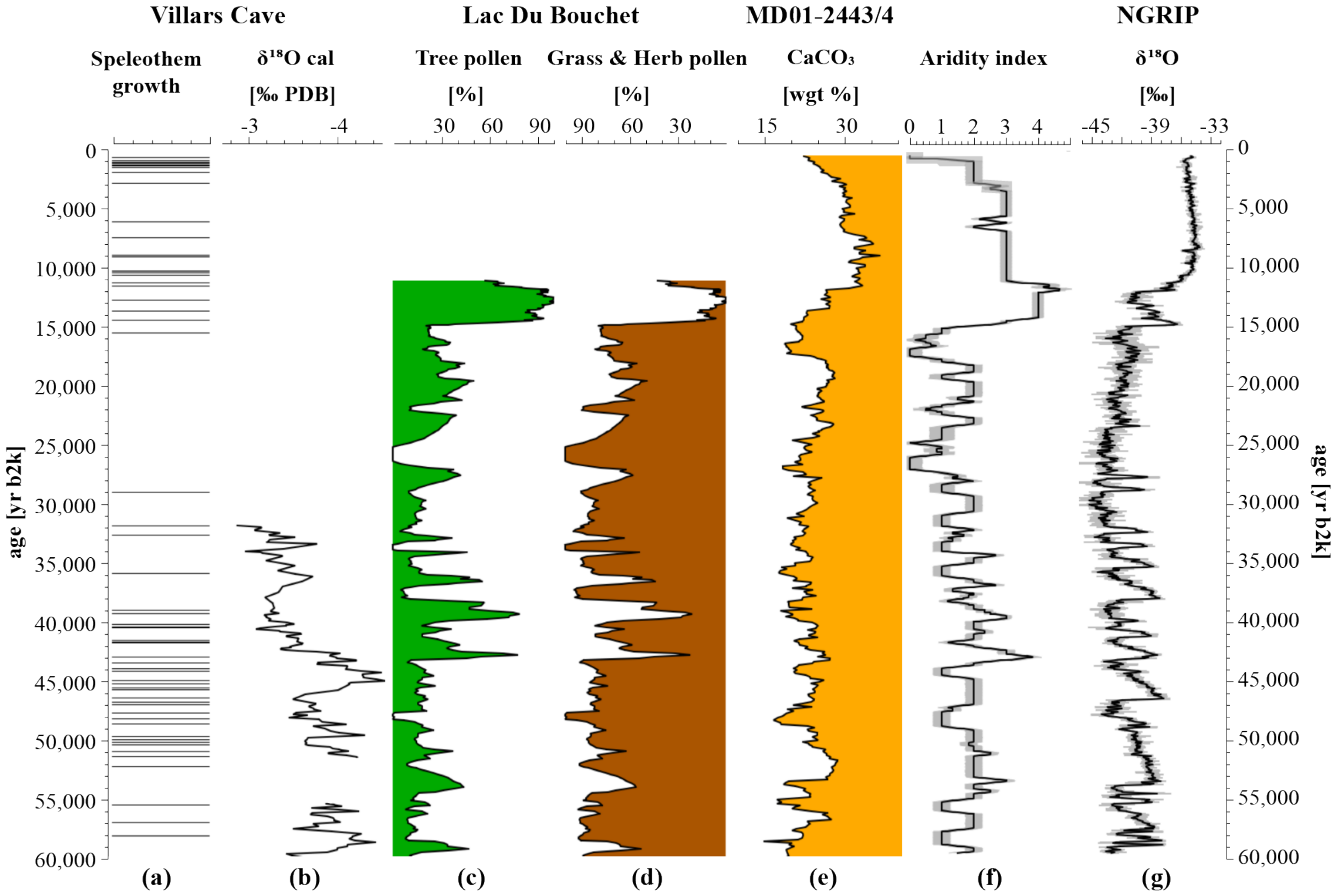

Figure S4: Southern European climate over the last 60 000 years: **(a)** Villars Cave (Genty et al., 2003, 2006; Labuhn et al., 2015; Wainer et al., 2009) show speleothem growth phases, which require mobile water from frequent precipitation; **(b)** $\delta^{18}O$ data with few apparent GIs comparable to **(g)**, more negative $\delta^{18}O$ values account for more humid conditions (Genty et al., 2003); **(c, d)** Lac Du Bouchet pollen data (Reille and de Beaulieu, 1990) are divided into tree- and herb & grass pollen. While trees require more precipitation, grasses are dominant for more arid conditions; **(e)** MD01-2443/4 marine cores $CaCO_3$ (Hodell et al., 2013) indicates more arid conditions with lower values, higher values account for more humid conditions; **(f)** Aridity index for Southern Europe as result from **(a-e),** for detailed information see method section; **(g)** $\delta^{18}O$ data from NGRIP ice core (North Greenland Ice Core Project Members et al., 2004) in comparison.

S5 Portuguese Margin:

The Portuguese margins sediment cores are known to be highly impacted by climate change on orbital and millennial timescales. Constant sedimentation rates are responsible for good stratigraphies and they are influenced by high- and low-latitude processes (Hodell et al., 2013). Today's mean annual temperatures are about 15 °C, winters are mild (10 - 13 °C) and summers are moderate (18 - 22 °C) with up to 3 000 mm yearly precipitation. Portuguese margin and Southern Europe contain the same dust record, the MD01-2443 sediment core shows dust in the $CaCO_3$ content. For Portuguese margin, a marine sediment core with terrestrial pollen input can be used to reconstruct the vegetation of the coast. Tree populations of sediment core MD95-2039 show rapid shifts, following GI-scheme. During Heinrich events 1 - 6, SST's dropped in order of 5 – 10 °C. Short GIs show less impact on the extend of woodland (Roucoux et al., 2005). Buraca Gloriosa Cave speleothems show the climate evolution of the last 220 000 years (Denniston et al., 2018). The cave is located 30 km from the Atlantic coast, near the both marine cores used for this region.

Within the timespan from 60 000 to 50 000 yr b2k (GIs 17-13), humid conditions can be reconstructed for Portuguese Iberian margin. Speleothem growth was continuous in Buraca Gloriosa Cave and shows high growth rates. The tree pollen in general were on a maximum during this time phase, showing high amplitude fluctuations between cooler and drier stadials and warmer and wetter interstadials (Roucoux et al., 2005), as well as a decline in dust content from 60 000 towards 50 000 yr b2k from relatively high values to lowest values until the Holocene. The high amount of tree pollen, speleothem growth and the decline in the dust content indicates a general warmer and wetter early MIS3 and consequently, low aridity with the begin of the phase and an intermediate aridity towards the end.

During the period from 50 000 to 32 000 yr b2k (GIs 12-5) an intermediate aridity is estimated for the region. H5 and H4 are visible within all records indicating a rapid climate change throughout the region. Speleothem growth rates were lower than before. Around H4 a hiatus of 41 000 to 36 000 years b2k in speleothem growth can be seen. Heinrich events 5 and 4 are strongly expressed within the MD95-2039 core indicating a dramatic decrease in climate conditions (Roucoux et al., 2005). A minor rise in dust is visible within the $CaCO_3$ content of MD01-2443 from in general intermediate dust values throughout this period for H5 and H4. Regarding all this, an intermediate aridity is estimated throughout this time phase with strong variability between interstadials and stadials for Portuguese margin region.

Between 32 000 and 15 000 yr b2k (GIs 4-2), the speleothem growth at Buraca Gloriosa Cave shows two hiatus during H3 and H1 (from 32 000 to 30 000 and 17 000 to 15 000). The amount of tree pollen was very low, open, herb-dominated steppic vegetation indicates cool and arid conditions. Less aridity towards the end of the phase is indicated from a slight increase in tree pollen and heath population, which required amelioration in climate (Roucoux et al., 2005). Intermediate dust values with a decrease towards the end are visible, again with stronger impressed Heinrich events compared to the other stadials. The LGM, which falls into this period, can be characterized by intermediate aridity but surprisingly low dust values towards the end.

The time phase from 15 000 yr b2k (GI1, YD) to present is marked by the onset of the Holocene with Bølling / Allerød. Speleothem growth restarted and remains constant until 10 000 yr b2k, a growth recovery from 3 000 to 1 000 yr b2k is also apparent. A rapid increase in tree pollen around 15 000 yr b2k marks a strong increase in temperature and precipitation. Younger Dryas cold event reduced that for a short duration, but afterwards the climate improved to Holocene and present day conditions. The dust values were highest during the begin of the time phase around 15 000 yr b2k and declines through the early Holocene temperature optimum. Aridity was very low with the begin of this phase but in the past 5 000 years, dust values increase again indicating higher aridity than during Altithermal.

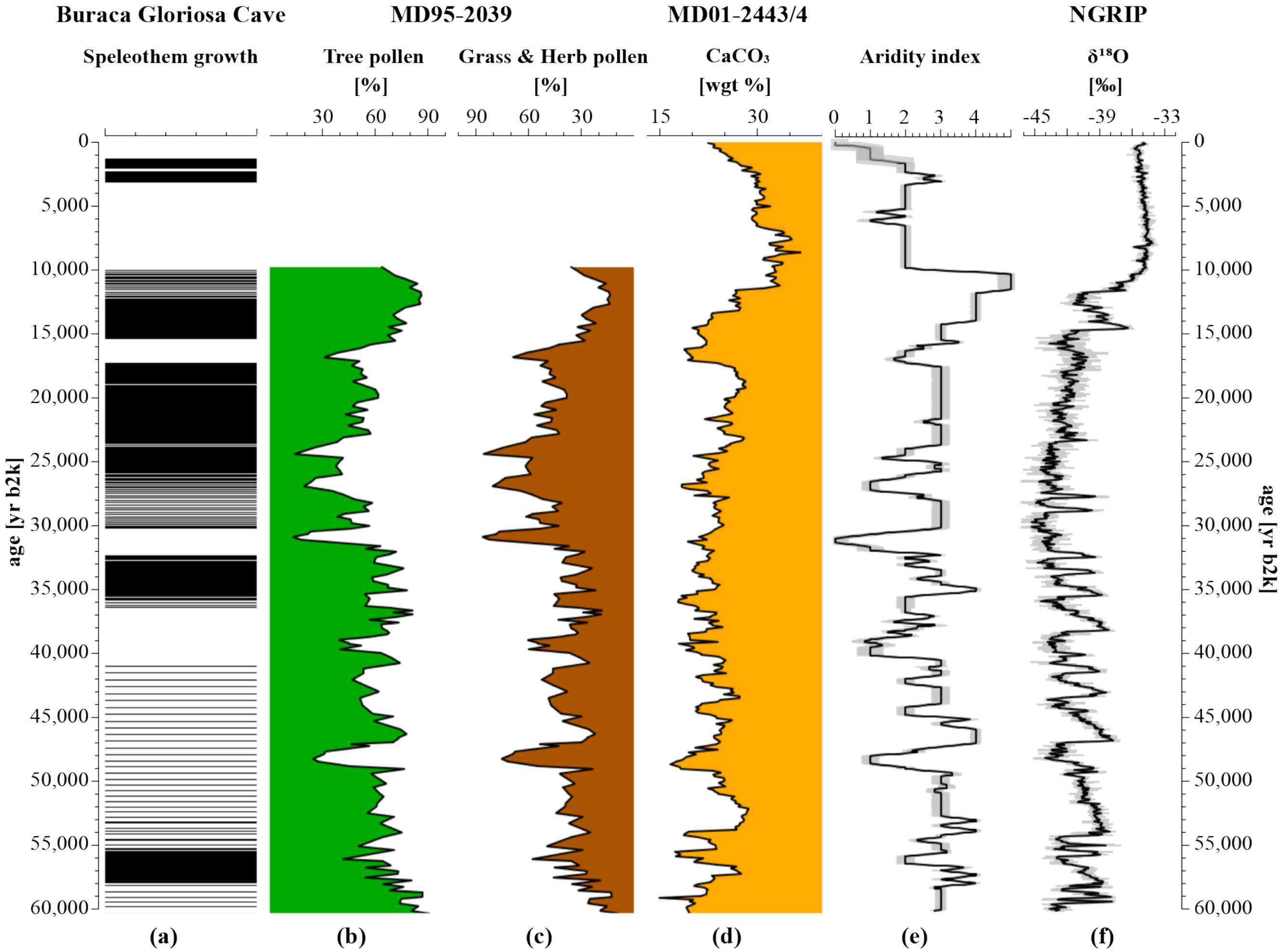

Figure S5: Portuguese margin climate over the last 60 000 years: **(a)** Buraca Gloriosa Cave (Denniston et al., 2018) show speleothem growth phases, which require mobile water from frequent precipitation; **(b, c)** MD95-2039 pollen data (Roucoux et al., 2005) are divided into tree- and herb & grass pollen. While trees require more precipitation, grasses are dominant for more arid conditions; **(d)** MD01-2443/4 marine cores $CaCO_3$ (Hodell et al., 2013) indicates more arid conditions with lower values, higher values account for more humid conditions; **(e)** Aridity index for Portuguese margin as result from **(a-d)**, for detailed information see method section; **(f)** $\delta^{18}O$ data from NGRIP ice core (North Greenland Ice Core Project Members et al., 2004) in comparison.

S6 Mediterranean Sea:

Southern Europe and the Mediterranean Sea region are known for hot and dry summers and mild and wet winters. The temperature average is about 18.9 °C and the total precipitation about 1000 mm/year with more precipitation in the western regions than in the eastern (Deutscher Wetterdienst, 2018). The archives for this synthesis are spread around the eastern Mediterranean region. The westernmost archive is the Lago Grande di Monticchio, a maar lake in Basilicata, southern Italy. The cores comprise climate information for the last 140 000 years (Allen et al., 1999; Brauer et al., 1999; Watts, 1985 and others) and completely varve counted, supplemented by a tephra chronology. The pollen from Monticchio show similar behaviour to the NGRIP indicating a closely coupled system between North Atlantic and the Mediterranean region (Allen et al., 1999; see Fig. S6). Speleothem growth occurs at several sites. Dim Cave in south western Turkey shows continuous speleothem growth from 12 000 yr b2k until 90 000 yr b2k with significant lower growth rates during glacial times (40 000 – 18 000 yr b2k, Ünal-İmer et al., 2015). A second speleothem from Soreq Cave in Israel shows continuous growth for the last 140 000 years. Two distinct isotopic events can be separated within the record within the last 60 000 years (Bar-Matthews et al., 1997, 2000). The dust record in M40/4_SL71 from SE Ionian Sea shows increased K/C ratio during arid conditions due to deflation of Kaolinite bearing dust, which was sedimented into basins during more humid conditions (Ehrmann et al., 2017). Kaolinite is a common mineral in North African dust and hence a useful dust tracer. During Heinrich events, the Mediterranean region was heavily arid and minor maxima of Kaolinite appear.

The timespan from 60 000 to 55 000 yr b2k comprises GIs 17 to 15. Speleothem growth occurs in Dim and Soreq Cave and $\delta^{18}O$ values are on relative highs around 57 000 yr b2k for both caves. The growth rates in Dim cave are lower than in younger parts of the speleothem. The amount of tree pollen is at intermediate values of 50 % and so is the K/C ratio, which shows H6 recorded in the sediment core at about 60 000 yr b2k. Overall, the aridity was at intermediate values.

GIs 14 to 9 are within the time of 55 000 to 40 000 yr b2k. The Dim Cave speleothem growth rate rises around 50 000 yr b2k, the $\delta^{18}O$ values sink, suggesting wetter climate. In addition, $\delta^{18}O$ was on peak value, which confirms the rapid. In Soreq Cave, $\delta^{18}O$ values where between 55 000 and 52 000 yr b2k higher and show similar conditions as today (Grant et al., 2012). Furthermore, Monticchio tree pollen are on a maximum during GI14 and GI12 (interpreted as pollen Assemblage Zones 13 and 11, see Allen et al., 1999). The core shows GI like appearance for this timespan. The dust record exhibits intermediate values with some minor peaks during stadial phases and H5 event. H4 is not visible due to a tephra layer within the event (Ehrmann et al., 2017). The precipitation was high during this time span considering fast speleothem growth, large amounts of tree pollen and intermediate dust values. The aridity index shows humid conditions, especially during interstadial times for this phase.

Glacial conditions are clearly visible between 40 000 and 17 200 yr b2k, with GIs 8 to 1. Speleothem growth is continuous through all time, but slowest during glacial at Dim Cave (Ünal-İmer et al., 2015). Soreq cave speleothem growth also continued showing variability in $\delta^{18}O$ on small scale with some minor peaks during GI3 and 4. The Monticchio pollen are low to medium on tree content during this time span with some variability. Higher tree pollen amount is present during interstadials and herbaceous taxa & steppe pollen increase in stadial times (Brauer et al., 2007). The K/C ratio shows H3 to H1 and is apart from that at intermediate values. The glacial time has frequent precipitation minima during Heinrich events and increased precipitation in times of interstadials. The aridity index remains on intermediate values during this time but showing climate ameliorations during interstadials.

Within the time span from 17 200 to 10 000 yr b2k are GI1 and the YD as well as the transition towards the Holocene. Speleothem growth at Dim and Soreq cave was fast and the $\delta^{18}O$ values increase in both speleothems. Tree pollen rapidly increase from glacial values of about 30 % to nearly 90 % after Bølling / Allerød. The YD is clearly visible in the SL71 dust record with increased K/C ratio. The aridity index increases strongly towards humid conditions during the early Holocene. During the Holocene (10 000 yr b2k to present) most of the records remain constant. Dim Cave speleothem did not grow anymore but $\delta^{18}O$ values from Soreq cave show consistent values with a variation between 8 500 and 7 000 yr b2k, where low $\delta^{18}O$ values indicate doubled precipitation and present day temperatures (Bar-Matthews et al., 1997). The amount of tree pollen stays constantly high with a small decrease to 75 % at about 2 000 yr b2k. The largest variation can be seen in the dust content, where the dust deflation reaches maximum values after the early Holocene optimum (EHTO). The large dust deflation, mainly originating from Sahara (Ehrmann et al., 2017), is consistent with the northward extension of the Saharan desert in modern times compared to early Holocene conditions (Jolly et al., 1998). The precipitation and temperature for the Mediterranean region within the Holocene was nearly at present day conditions while the African continent underwent a huge change.

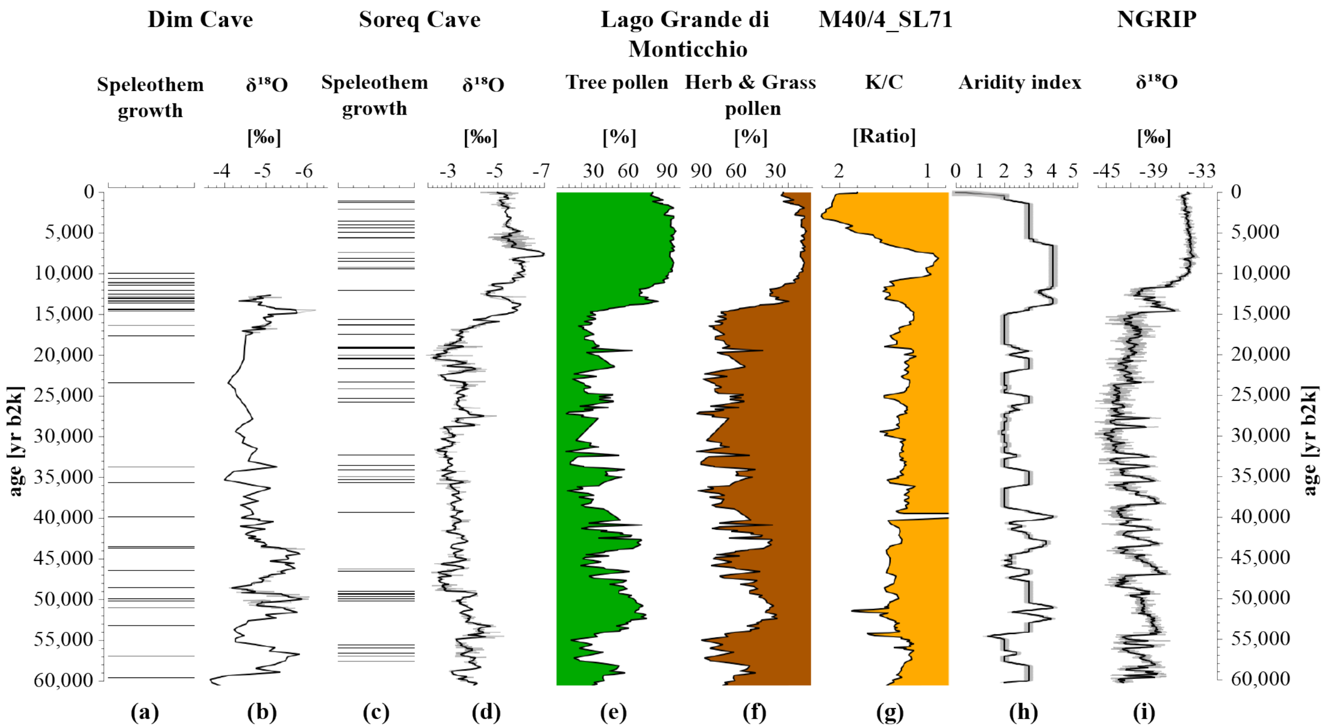

Figure S6: Mediterranean Sea climate over the last 60 000 years: Dim Cave (Ünal-İmer et al., 2015) **(a, b)** and Soreq Cave (Bar-Matthews et al., 2000; Grant et al., 2012) **(c, d)** show speleothem growth phases, which require mobile water from frequent precipitation; **(b, d)** $\delta^{18}O$ data with few apparent GIs comparable to **(j)**, more negative $\delta^{18}O$ values account for more humid conditions; **(e, f)** Lago Grande di Monticchio pollen data (Brauer et al., 2007) are divided into tree- and herb & grass pollen. While trees require more precipitation, grasses are dominant for more arid conditions; **(g)** Dust reconstruction from M40/4_SL71 marine core K/C ratio (Ehrmann et al., 2017) indicates more arid conditions with higher values, lower values account for more humid conditions; **(h)** Aridity index for Mediterranean Sea region as reconstructed from **(a, c, e, g).** For detailed information see method section; **(i)** $\delta^{18}O$ data from NGRIP ice core (North Greenland Ice Core Project Members et al., 2004) in comparison.

S7 Santa Barbara basin:

The region of the Santa Barbara basin is well known for its brief interstadial events of the past 60 000 years. The basin is located at the inner continental border of Southern California with a depth of about 600 m and contains oxygen-depleted water below 475 m (Behl, 1995; Behl and Kennett, 1996; Heusser, 1998). Due to this depletion zone, an excellent preservation of sediment material, pollen and warves occurs within the ODP-893A. In the benthic foraminifer record of ODP-893A (Cannariato et al., 1999) all GIs are visible as in the $\delta^{18}O$ record of the NGRIP ice core. About 800 km east of the Santa Barbara basin the “Cave of the Bells” speleothem in Arizona is located (Wagner et al., 2010). Aridity in the southwestern USA and climate information stored in the NGRIP show a similar pattern of fast interstadial / stadial changes. Cooler temperatures in high latitudes are connected to increased moisture in this region. Hence, higher $\delta^{18}O$ values were interpreted as warmer temperatures corresponding to drier winters (Wagner et al., 2010). Also, a speleothem of the “Fort Stanton Cave” in New Mexico can help to understand variabilities within the region and shows the GIs 1-12 (Asmerom et al., 2010). No larger dust deflation is known for that region, hence no paleodust record can be used within the synthesis. The climate today is as in Mediterranean regions with temperatures between 9.9 °C and 18,6 °C and a precipitation of about 600 mm/year (NOAA-NCDC weather service, 2018).

Between 60 000 and 48 000 years b2k (early MIS3, GIs 17-13) a high amount of tree pollen of about 80 % indicates high temperatures and at least moderate precipitation (see Fig. S7). The benthic foraminifers show high abundances, which is interpreted as an interstadial signal (Cannariato et al., 1999). Bells Cave speleothems show growth starting at about 54 000 years b2k. The $\delta^{18}O$ values of -9 ‰ indicate warm temperatures and moderate precipitation. Similarly, the Fort Stanton speleothem also shows high $\delta^{18}O$ values up to -5.5 ‰ during early MIS3 period. This time was characterized by warm temperatures and intermediate precipitation.

The timespan from 48 000 to 27 540 yr b2k comprises the GIs 12 to 3. All of them are visible in the foraminifer content as well as in the Fort Stanton speleothem. The Cave of the Bells speleothem comprises a hiatus between 24 000 and 29 000 yr b2k so that GI2 to 4 are missing within that record. The precipitation and temperature vary from interstadials to stadials, but the amount of tree pollen stays relatively constant at around 80 %. That indicates, the range of temperature and precipitation change did not pass a threshold on which an abrupt vegetational change would have occurred and temperatures and precipitation stayed close to early MIS3 conditions in respect to the stadial / interstadial changes.

From 27 540 to 14 700 yr b2k (onset of the Bølling / Allerød) the time is characterized by a drop of the Dysoxic benthic foraminifer content to low values between 0 and 15 % in contrast to the continuous high amount of tree pollen before. The Bells Cave speleothem’s hiatus continues until 24 000 yr b2k and growth started again with the onset of GI-2 (23 340 yr b2k), also visible in the foraminifer content. Speleothem growth at the Fort Stanton speleothem was continuous during this time span. The combination of all proxies shows cooler temperatures and increased moisture for the Santa Barbara basin during this period.

The Holocene part from the onset of Bølling / Allerød (B/A, 14 700 yr b2k) until present shows the YD in all records, but the records end around 10 000 yr b2k. Both speleothems show lower $\delta^{18}O$ values as well as ODP-893A low dysoxic foraminifer contents. The vegetational record shows a decrease in tree pollen and a corresponding increase in grass pollen. Most recently, the speleothems and the ODP-893A foraminifer records show the start of the Holocene at 11 700 yr b2k by increased values indicating warmer climate. The precipitation increases drastically with sinking tree pollen amount (Heusser, 1998) towards the Holocene. Due to a lack of a dust record, continuous speleothem growth and insignificant changes in the amount of tree pollen, the aridity index for this region is inconclusive and constantly at intermediate values. Therefore, the Aridity index calculation for this region ends around 10 000 yr b2k.

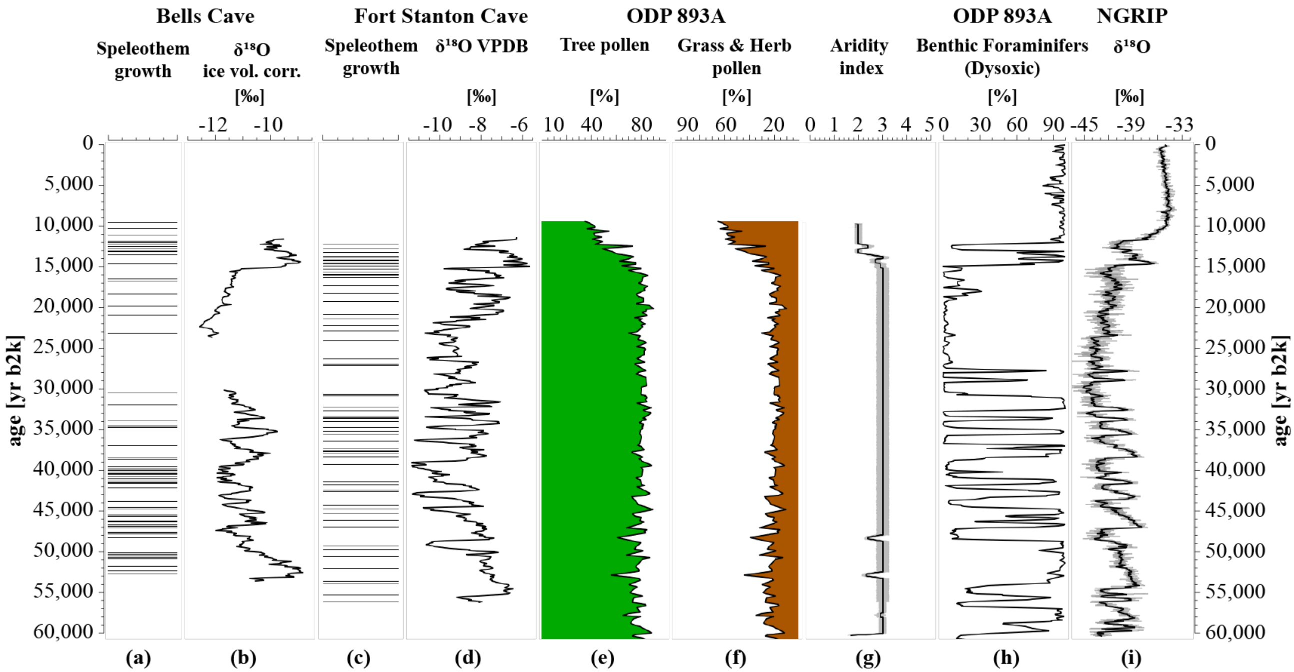

Figure S7: Santa Barbara Basin climate over the last 60 000 years: Bells Cave (Wagner et al., 2010) **(a, b)** and Fort Stanton (Asmerom et al., 2010) **(c, d)** show speleothem growth phases, which require mobile water from frequent precipitation; **(b, d)** $\delta^{18}O$ data with few apparent GIs comparable to **(h)** and **(j)**, more positive $\delta^{18}O$ values account for increased precipitation; **(e, f)** ODP893A marine core pollen data (Heusser, 1998) are divided into tree- and herb & grass pollen. While trees require more precipitation, grasses are dominant for more arid conditions; **(g)** Aridity index for St. Barbara Basin region as result from **(a, c, e).** For detailed information see method section; **(h)** Dysoxic Benthic Foraminifer data from marine core ODP893A (Cannariato et al., 1999) with distinguishable GIs in comparison to speleothem and NGRIP $\delta^{18}O$ data **(b, d, i)**; **(i)** $\delta^{18}O$ data from NGRIP ice core (North Greenland Ice Core Project Members et al., 2004) in comparison.

S 8 Global tree pollen pattern

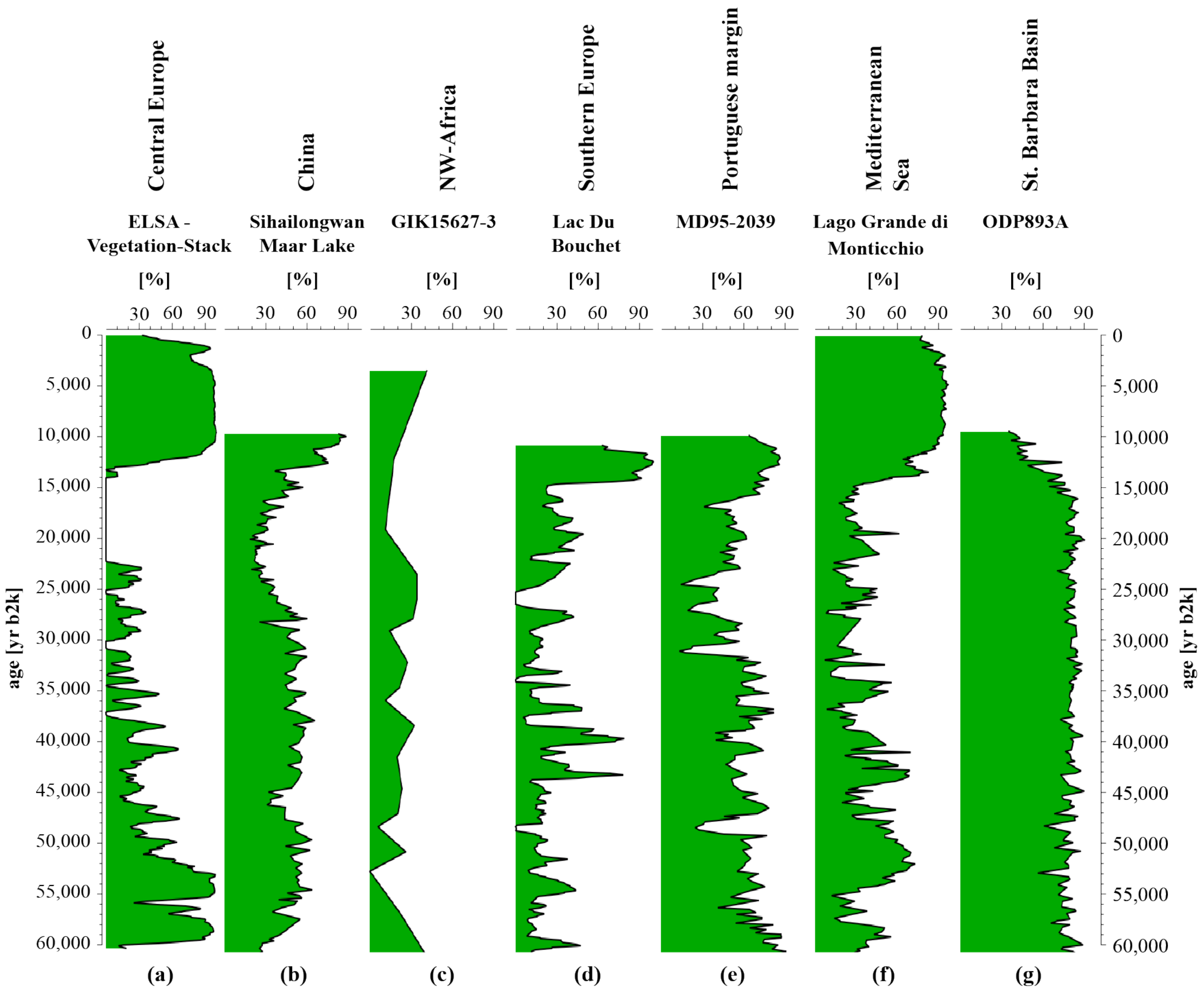

Figure S87: Global tree pollen records for the last 60 000 years. Higher amounts of tree pollen indicate increased humidity. **(a)** Central European ELSA-Vegetation-Stack (Sirocko et al., 2016); **(b)** Chinese Sihailongwan Maar Lake (Mingram et al., 2018); **(c)** North-West Africa marine core GIK15627-3 (Hooghiemstra et al., 1992); **(d)** Southern Europe Lac Du Bouchet (Reille and de Beaulieu, 1990); **(e)** Portuguese margin marine core MD95-2039 (Roucoux et al., 2005); **(f)** Lago Grande di Monticchio for Mediterranean Sea region (Brauer et al., 2007); **(g)** St. Barbara Basin marine core ODP893A (Heusser, 1998)

Figure S8 shows all tree pollen of this synthesis. Only three regions worldwide encompass sediment cores with pollen data for the whole last 60 000 years. The ELSA-Vegetation-Stack for Central Europe (Sirocko et al., 2016) consists of the sediment cores from Holzmaar and Dehner Maar, which cover the last 60 000 years in total. The Mediterranean record from 'Lago Grande di Monticchio' also covers this time as well as pollen from the Sihailongwan Maar Lake (China). However, Sihailongwan Maar Lake pollen profiles of Mingram (Mingram et al., 2018) and Stebich (Stebich et al., 2015) diverge for

Holocene and need to be adjusted. Pollen records for the Arabian Sea region are not available. The pollen assemblage of St. Barbara Basin is on very high values throughout the whole record due to sedimentation pattern in the marine basin as regional effects (Heusser, 1995, 1998).

Early MIS3 phase shows tree pollen maxima for the following regions: Central Europe, China, Portuguese margin and Mediterranean Sea. Although, the timings of the pollen maxima are not synchronous, enhanced precipitation and humidity for early MIS3 can be stated for these regions. The tree pollen show impairing climate conditions during late MIS3 towards LGM conditions. A well expressed LGM is visible in the pollen archives of Central Europe, China, Southern Europe, Portuguese margin and the Mediterranean. The LGM was mainly arid for all regions. The following transition towards the Holocene with the onset of Bølling / Allerød (14 700 yr b2k) is visible in all pollen records by massive changes in the tree pollen content. St. Barbara Basin shows decreasing pollen values (see S7). All other regions show increasing tree pollen amounts indicating more humid conditions and climate amelioration for the early Holocene.

S9 Stratigraphies and age / depths relations

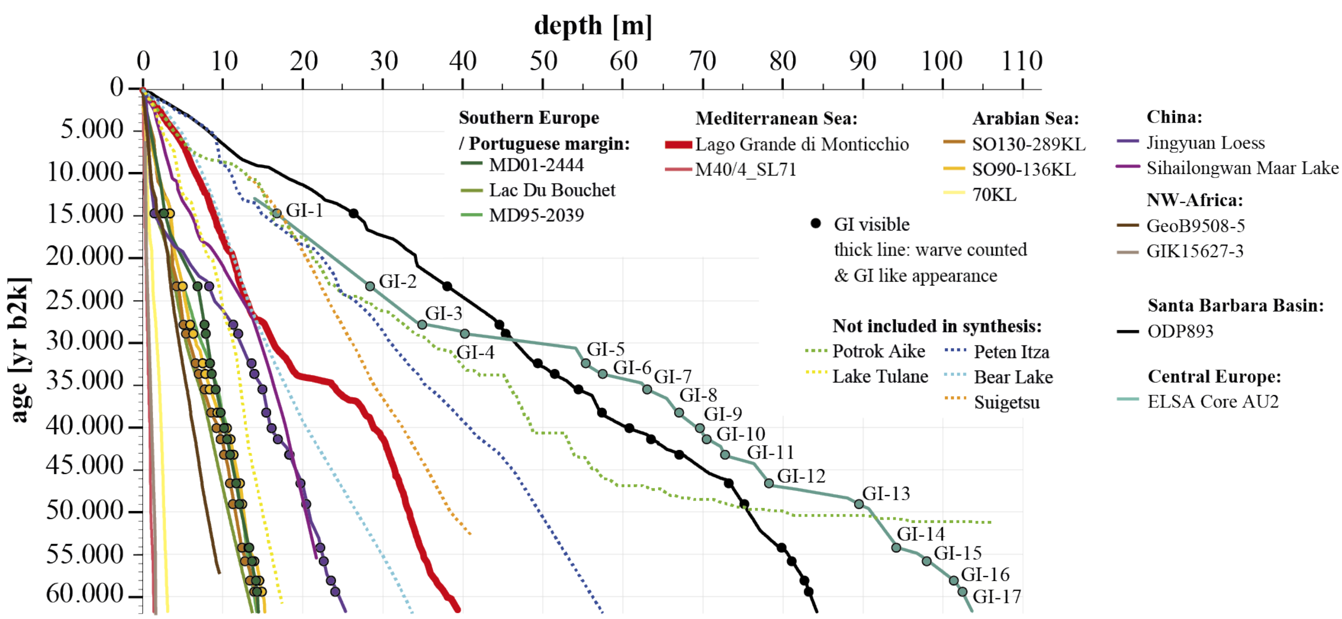

Figure S9: Global age / depths relations of various sediment cores. Solid lines show cores used for this synthesis. Thick red line shows Lago Grande di Monticchio, which is warve counted and shows GI like appearance. Points show apparent GIs. Dotted lines give other well-known high resolution records not included in this synthesis. For references of included cores see chapter 2 and S1-S7; Potrok Aike, Southern Patagonia, Argentina (Kliem et al., 2013); Lake Tulane, Florida, USA (Grimm et al., 2006); Petén-Itzá, Guatemala (Correa-Metrio et al., 2012); Bear Lake, Utah-Idaho, USA (Jiménez-Moreno et al., 2007); Lake Suigetsu, Japan (Bronk Ramsey et al., 2012).

Stratigraphical uncertainties are the major sources of error for this synthesis. All stratigraphies of original publications remained unchanged, apart from referring all records to years b2k (before the year 2000 CE). Different dating methods in general have various uncertainties. Archives of this synthesis were dated by ^{14}C ages, optically stimulated luminescence (OSL), U/Th dating of speleothems, varve counting, tuning to NGRIP or marine isotope stack, paleomagnetismus correlation, tephra chronology or cross correlating (see Tab. S1). Age uncertainties of speleothem U/Th dating range between 1 and 4 %, resulting in the most reliable ages for speleothems. ^{14}C calibrations were greatly improved and e.g. Hughen et al. (2006) has calibrated the ^{14}C curves with the absolutely dated Hulu speleothems. Nevertheless, ^{14}C ages of this synthesis bear maximum errors up to 12 % - or up to 7 000 years. Error values of OSL dating range up to 10 % or about 5 000 years for the last 60 000 years. Warve counting errors depend strongly on the sedimentation rate of the archive, but error values can stack up to 5 000 years as well. For NGRIP tuning, age uncertainties of the ice core are minimized by several dating approaches and stack up to 2 500 years for the last 60 000 years. To sum it up, no definitive ages for the previously described turning point can be determined from this work. Nevertheless, synchronous patterns occurred during climate history and the estimated ages give a good evaluation of the turning points of the precipitation.

The sampling resolution of the records is also extremely important. More samples and analyses result in a much more detailed explanations and interpretations for the records. High frequency sampling, especially in sediment cores is mainly depending on the sedimentation rate. Figure S9 shows all sediment archives and records of this work with the age-depths relation. The thick, red line accounts for the warve-counted Lago Grande di Monticchio core. Points indicate GI appearance in the marine records of Santa Barbara Basin (ODP893), Chinese Loess (Jingyuan Loess sequence), Arabian Sea (SO-136KL) and Portuguese margin (MD01-2444) and Lake sediments of Central Europe (ELSA-Dust-Stack). The highest sedimentation rates during the last 60 000 years can be found in Santa Barbara Basin and ELSA-AU2 core with about 1-2 mm/year.

Several other high resolution records with extend into MIS3 (Fig. S9, dotted lines) are published but not used for this synthesis. They are additionally shown for comparison and completeness. These cores were too far away from the chosen key regions to fit into a proper synthesis or do not extend until the begin of MIS3 (60 000 yr b2k). However, these cores are good climate archives with striking sedimentation rates of 0.26 mm/yr (Lake Tulane), 0.5 mm/yr (Bear Lake), 0.75 mm/yr (Lake Suigetsu) up to Petén-Itzá (~1 mm/yr) and Potrok Aike (~1.6 mm/yr) and should be mentioned within this synthesis.

S10 Matlab code for error calculation:

```
%Aridity Index simulation
%input here your estimated error as [%]:
fehlerSp=2;
fehlerPo=3;
fehlerDu=5;

%read the CSV data without headlines. "," separated
m = csvread('filename_template.csv');

%Separate on columns
%m3=m(:,3)
%m4=m(:,4)
%m5=m(:,5)

mat=zeros(3,1201,100);
%mat(:,1)=m3

for k=1:3

    for i=1:100
        mat(k,:,i)=m(:,k+2);
    end
end

% fill matrix with random numbers
for a=1:1201
    nSp=mod(mat(1,a,1)+1,2);
    for i=1:fehlerSp
       mat(1,a,i)= nSp;
    end

    nPo=mat(2,a,1);
    if nPo==1
        for i=1:fehlerPo/2
            mat(2,a,i)=0;
        end

        for j=i:fehlerPo
            mat(2,a,j)=2;
        end
    else
        for i=1:fehlerPo
            mat(2,a,i)=1;
        end
    end

    nDu=mat(3,a,1);
    if nDu==1
```

```
        for i=1:fehlerDu/2
            mat(3,a,i)=0;
        end

        for j=i:fehlerDu
            mat(3,a,j)=2;
        end
    else
        for i=1:fehlerDu
            mat(3,a,i)=1;
        end
    end

end

%simulation starts here-->
%number of simulations
noRuns = 100000;

%Std Matrix erstellen
sims=zeros(noRuns,1201);

for sIndex=1:noRuns
    %1201 Random Werte zwischen 0 und 2
    r1 = ceil(rand(1201,1)*100);

    %recalculate index from mat
    vec_speleothem=zeros(1,1201);
    vec_pollen=zeros(1,1201);
    vec_dust=zeros(1,1201);

    for i=1:1201
        vec_speleothem(i)=mat(1,i,r1(i));
        vec_pollen(i)=mat(2,i,r1(i));
        vec_dust(i)=mat(3,i,r1(i));
    end

    tmp =(vec_speleothem+vec_pollen+vec_dust);
    sims(sIndex,:) =tmp;
end

result=zeros(1201:1);

%stadtad deviation for each value individually
for k=1:1201
    result(k) = std(sims(:,k));
end
resultTransp=result.';
csvwrite('error_template_name.txt',resultTransp);
```

Region	Archive	Proxy type	Location	Time covered [ka b2k]	Dating method	Reference
	Speleothem	Speleothem	Bunker Cave	0 - 52	1, 2	Fohlmeister et al., 2012, 2013; Weber et al., 2018
Central Europe	Speleothem	Speleothem	Spannagel Cave	0 - 275	1	Holzkämper et al. 2005; Spötl & Mangini, 2002, 2012
	Lake Sediment core	Pollen	Dehner Maar & Holzmaar	0 - 63	2, 3, 4, 5	Sirocko et al., 2016
	Lake Sediment core	Dust	Dehner Maar	0 - 130	2, 6, 5	Seelos et al., 2009
	Speleothem	Speleothem	Socotra Cave	2 - 5; 40 - 54	1	Fleitmann et al., 2007 and refs. within; Burns et al., 2003
	Speleothem	Speleothem	Oman Caves	0 - 11	1	Fleitmann et al., 2007 and refs. within
Arabian Sea	Marine Sediment core	Dust	Western Arabian Sea	0 - 135	2, 4, 7	Leuschner & Sirocko, 2003
	Marine Sediment core	TOC	Western Arabian Sea	0 - 65	2, 4, 8	Schulz et al., 1998
	Marine Sediment core	Reflectance	Western Arabian Sea	0 - 80	2, 5	Deplazes et al., 2014
	Speleothem	Speleothem	Grotte de Piste	5 - 12	1	Wassenburg et al., 2012, 2016
NW-Africa	Speleothem	Speleothem	Grotte Prison de Chien	3 - 97	1	Wassenburg et al., 2012
	Marine Sediment core	Pollen	West off Morocco	6 - 250	2, 8	Hooghiemstra et al., 1992
	Marine Sediment core	Dust	West off Senegal	0 - 57	2, 8	Collins et al., 2013 and refs. within
	Speleothem	Speleothem	Hulu Cave	11 - 75	1, 8	Wang et al., 2001; Liu et al., 2010
China	Lake Sediment core	Pollen	Sihailongwan Maar Lake	0 - 65	2, 3, 4	Mingram et al., 2018
	Lake Sediment core	Pollen	Sihailongwan Maar Lake	0 - 12	2	Stebich et al., 2015
	Loess profile	Dust	Jingyuan Loess	0 - 80	5, 6, 9	Sun et al., 2010
	Speleothem	Speleothem	Villars Cave	5 - 15; 32 - 83	1	Genty et al., 2006; Genty et al., 2003
	Speleothem	Speleothem	Villars Cave	0 -3	1	Labuhn et al., 2015
Southern Europe	Speleothem	Speleothem	Villars Cave	28 - 51; 11 - 178	1	Wainer et al., 2009; 2011
	Lake Sediment core	Pollen	Lac Du Bouchet	15 - 68	2, 10	Reille & Beaulieu, 1989;
	Marine Sediment core	Dust	MD01-2443/4	0 - 420	2, 5, 7, 8, 9	Hodell et al., 2013, Barker et al., 2011
	Speleothem	Speleothem	Buraca Gloriosa Cave	0 - 220	1	Denniston et al., 2018
Portuguese margin	Marine Sediment core	Pollen	MD95-2039	0 - 65	2, 5, 9	Roucoux et al., 2005, Vogelsang, E., 2001
	Marine Sediment core	Dust	MD01-2443/4	0 - 420	2, 5, 7, 8, 9	Hodell et al., 2013, Barker et al., 2011
	Speleothem	Speleothem	Dim Cave	5 - 85	1	Ünal-Imer et al., 2015
	Speleothem	Speleothem	Soreq Cave	0 - 150	1	Grant et al., 2012
Mediterranean Sea	Speleothem	Speleothem	Soreq Cave	0 - 140	1	Bar-Matthews et al., 2000
	Lake Sediment core	Pollen	Lago Grande di Monticchio	0 - 130	2, 3, 9	Brauer et al., 2007
	Marine Sediment core	Dust	MD40/4_SL71	0 - 180	2, 4, 8	Ehrmann et al., 2017
	Speleothem	Speleothem	Bells Cave	8 - 53	1	Wagner et al., 2010
St. Barbara Basin	Speleothem	Speleothem	Fort Stanton	11 - 57	1	Asmerom et al., 2010
	Marine Sediment core	Pollen	ODP 893A	9 - 135	2, 8, 9	Heusser, 1998
	Marine Sediment core	Foraminifers ∂18O	ODP 893A	0 - 60	2, 8, 9	Cannariato et al, 1999
Greenland	Ice Core	$\partial^{18}O$	NGRIP	0 - 105	3	NGRIP Members et al., 2004
Antarctica	Ice Core	$\partial^{18}O$	WAIS Divide	0 - 68	3	WAIS Divide Project Members, 2015

Table S1: Paleoclimatic records used in this synthesis. Records with grey background are not included into the generation of the aridity index. Dating methods: 1 Th/U-dating; 2 ^{14}C-Radiocarbon dating; 3 Varve counting; 4 Tephrachronology; 5 Ice core tuning; 6 OSL Luminescence dating; 7 Orbital tuning; 8 Oxygen isotope tuning; 9 Cross correlation; 10 Paleomagnetic correlation

References:

Allen, J. R. M., Brandt, U., Brauer, A., Hubberten, H.-W., Huntley, B., Keller, J., Kraml, M., Mackensen, A., Mingram, J., Negendank, J. F. W., Nowaczyk, R., Oberhänsli, H., Watts, W. A., Wulf, S. and Zolitschka, B.: Rapid environmental changes in southern Europe during the last glacial period, Nature, 400, 740–743, 1999.

Antoine, P., Rousseau, D.-D., Zöller, L., Lang, A., Munaut, A.-V., Hatté, C. and Fontugne, M.: High-resolution record of the last Interglacial–glacial cycle in the Nussloch loess–palaeosol sequences, Upper Rhine Area, Germany, Quaternary International, 76–77, 211–229, doi:10.1016/S1040-6182(00)00104-X, 2001.

Asmerom, Y., Polyak, V. J. and Burns, S. J.: Variable winter moisture in the southwestern United States linked to rapid glacial climate shifts, Nature Geoscience, 3(2), 114–117, doi:10.1038/ngeo754, 2010.

Bar-Matthews, M., Ayalon, A. and Kaufman, A.: Late Quaternary Paleoclimate in the Eastern Mediterranean Region from Stable Isotope Analysis of Speleothems at Soreq Cave, Israel, Quaternary Research, 47(2), 155–168, doi:10.1006/qres.1997.1883, 1997.

Bar-Matthews, M., Ayalon, A. and Kaufman, A.: Timing and hydrological conditions of Sapropel events in the Eastern Mediterranean, as evident from speleothems, Soreq cave, Israel, Chemical Geology, 169(1–2), 145–156, 2000.

Behl, R. J.: Sedimentary facies and sedimentology of the late quaternary Santa Barbara basin, site 893, , 146–2, doi:10.2973/odp.proc.sr.146-2.1995, 1995.

Behl, R. J. and Kennett, J. P.: Brief interstadial events in the Santa Barbara basin, NE Pacific, during the past 60 kyr, Nature, 379, 243, 1996.

Brauer, A., Endres, C. and Negendank, J. F. W.: Lateglacial calendar year chronology based on annually laminated sediments from Lake Meerfelder Maar, Germany, Quaternary International, 61(1), 17–25, doi:10.1016/S1040-6182(99)00014-2, 1999.

Brauer, A., Allen, J. R. M., Mingram, J., Dulski, P., Wulf, S. and Huntley, B.: Evidence for last interglacial chronology and environmental change from Southern Europe, Proceedings of the National Academy of Sciences, 104(2), 450–455, doi:10.1073/pnas.0603321104, 2007.

Bronk Ramsey, C., Staff, R. A., Bryant, C. L., Brock, F., Kitagawa, H., van der Plicht, J., Schlolaut, G., Marshall, M. H., Brauer, A., Lamb, H. F., Payne, R. L., Tarasov, P. E., Haraguchi, T., Gotanda, K., Yonenobu, H., Yokoyama, Y., Tada, R. and Nakagawa, T.: A Complete Terrestrial Radiocarbon Record for 11.2 to 52.8 kyr B.P., Science, 338(6105), 370–374, doi:10.1126/science.1226660, 2012.

Burns, S. J., Fleitmann, D., Matter, A., Kramers, J. and Al-Subbary A. A: Indian Ocean Climate and a Absolute Chronology over Dansgaard/Oescher Events 9 to 13, Science, 301, 1365–1367, 2003.

Cannariato, K. G., Kennett, J. P. and Behl, R. J.: Biotic response to late Quaternary rapid climate switches in Santa Barbara Basin: Ecological and evolutionary implications, Geology, 27(1), 63, doi:10.1130/0091-7613(1999)027<0063:BRTLQR>2.3.CO;2, 1999.

Collins, J. A., Govin, A., Mulitza, S., Heslop, D., Zabel, M., Hartmann, J., Röhl, U. and Wefer, G.: Abrupt shifts of the Sahara-

Sahel boundary during Heinrich stadials, Climate of the Past, 9(3), 1181–1191, doi:10.5194/cp-9-1181-2013, 2013.

Correa-Metrio, A., Bush, M. B., Hodell, D. A., Brenner, M., Escobar, J. and Guilderson, T.: The influence of abrupt climate change on the ice-age vegetation of the Central American lowlands: Abrupt climate change in ice-age Central America, Journal of Biogeography, 39(3), 497–509, doi:10.1111/j.1365-2699.2011.02618.x, 2012.

Denniston, R. F., Houts, A. N., Asmerom, Y., Wanamaker Jr., A. D., Haws, J. A., Polyak, V. J., Thatcher, D. L., Altan-Ochir, S., Borowske, A. C., Breitenbach, S. F. M., Ummenhofer, C. C., Regala, F. T., Benedetti, M. M. and Bicho, N. F.: A stalagmite test of North Atlantic SST and Iberian hydroclimate linkages over the last two glacial cycles, Climate of the Past, 14(12), 1893–1913, doi:https://doi.org/10.5194/cp-14-1893-2018, 2018.

Deplazes, G., Lückge, A., Stuut, J.-B. W., Pätzold, J., Kuhlmann, H., Husson, D., Fant, M. and Haug, G. H.: Weakening and strengthening of the Indian monsoon during Heinrich events and Dansgaard-Oeschger oscillations: INDIAN MONSOON DURING HEINRICH EVENTS, Paleoceanography, 29(2), 99–114, doi:10.1002/2013PA002509, 2014.

Deutscher Wetterdienst: Wetter und Klima - Deutscher Wetterdienst - Klimadaten weltweit, [online] Available from: https://www.dwd.de/DE/leistungen/klimadatenwelt/klimadatenwelt_node.html (Accessed 17 July 2018), 2018.

Ehrmann, W., Schmiedl, G., Beuscher, S. and Krüger, S.: Intensity of African Humid Periods Estimated from Saharan Dust Fluxes, edited by S.-P. Xie, PLOS ONE, 12(1), e0170989, doi:10.1371/journal.pone.0170989, 2017.

Fleitmann, D., Burns, S. J., Mangini, A., Mudelsee, M., Kramers, J., Villa, I., Neff, U., Al-Subbary, A. A., Buettner, A., Hippler, D. and Matter, A.: Holocene ITCZ and Indian monsoon dynamics recorded in stalagmites from Oman and Yemen (Socotra), Quaternary Science Reviews, 26(1–2), 170–188, doi:10.1016/j.quascirev.2006.04.012, 2007.

Genty, D., Blamart, D., Ouahdi, R., Gilmour, M., Baker, A., Jouzel, J. and Van-Exter, S.: Precise dating of Dansgaard–Oeschger climate oscillations in western Europe from stalagmite data, Nature, 421(6925), 833–837, doi:10.1038/nature01391, 2003.

Genty, D., Blamart, D., Ghaleb, B., Plagnes, V., Causse, Ch., Bakalowicz, M., Zouari, K., Chkir, N., Hellstrom, J. and Wainer, K.: Timing and dynamics of the last deglaciation from European and North African δ13C stalagmite profiles—comparison with Chinese and South Hemisphere stalagmites, Quaternary Science Reviews, 25(17–18), 2118–2142, doi:10.1016/j.quascirev.2006.01.030, 2006.

Grant, K. M., Rohling, E. J., Bar-Matthews, M., Ayalon, A., Medina-Elizalde, M., Ramsey, C. B., Satow, C. and Roberts, A. P.: Rapid coupling between ice volume and polar temperature over the past 150,000 years, Nature, 491(7426), 744–747, doi:10.1038/nature11593, 2012.

Grimm, E. C., Watts, W. A., Jacobson Jr., G. L., Hansen, B. C. S., Almquist, H. R. and Dieffenbacher-Krall, A. C.: Evidence for warm wet Heinrich events in Florida, Quaternary Science Reviews, 25(17–18), 2197–2211, doi:10.1016/j.quascirev.2006.04.008, 2006.

Heusser, L.: Pollen stratigraphy and paleoecologic interpretation of the last 160 kyr from Santa Barbara Basin, ODP Hole 893A, in Proc. Ocean Drill. Program Sci. Results, vol. 146, edited by J. Kennett, J. G. Baldauf, and M. Lyle, pp. 265–279., 1995.

Heusser, L.: Direct correlation of millennial-scale changes in western North American vegetation and climate with changes in the California Current System over the past ~60 kyr, Paleoceanography, 13(3), 252–262, doi:10.1029/98PA00670, 1998.

Hodell, D., Crowhurst, S., Skinner, L., Tzedakis, P. C., Margari, V., Channell, J. E. T., Kamenov, G., Maclachlan, S. and Rothwell, G.: Response of Iberian Margin sediments to orbital and suborbital forcing over the past 420 ka, Paleoceanography, 28(1), 185–199, doi:10.1002/palo.20017, 2013.

Hooghiemstra, H., Stalling, H., Agwu, C. O. C. and Dupont, L. M.: Vegetational and climatic changes at the northern fringe of the sahara 250,000–5000 years BP: evidence from 4 marine pollen records located between Portugal and the Canary Islands, Review of Palaeobotany and Palynology, 74(1), 1–53, doi:10.1016/0034-6667(92)90137-6, 1992.

Hughen, K., Southon, J., Lehman, S., Bertrand, C. and Turnbull, J.: Marine-derived 14C calibration and activity record for the past 50,000 years updated from the Cariaco Basin, Quaternary Science Reviews, 25(23–24), 3216–3227, doi:10.1016/j.quascirev.2006.03.014, 2006.

Jiménez-Moreno, G., Anderson, S. R. and Fawcett, P.: Orbital- and millennial-scale vegetation and climate changes of the past 225ka from Bear Lake, Utah–Idaho (USA), Quaternary Science Reviews, 26(13–14), 1713–1724, doi:10.1016/j.quascirev.2007.05.001, 2007.

Jolly, D., Harrison, S. P., Damnati, B. and Bonnefille, R.: Simulated Climate and Biomes of Africa During the Late Quaternary: Comparison with Pollen and Lake Status Data, Quaternary Science Reviews, 17, 29, 1998.

Kliem, P., Enters, D., Hahn, A., Ohlendorf, C., Lisé-Pronovost, A., St-Onge, G., Wastegård, S. and Zolitschka, B.: Lithology, radiocarbon chronology and sedimentological interpretation of the lacustrine record from Laguna Potrok Aike, southern Patagonia, Quaternary Science Reviews, 71, 54–69, doi:10.1016/j.quascirev.2012.07.019, 2013.

Labuhn, I., Genty, D., Vonhof, H., Bourdin, C., Blamart, D., Douville, E., Ruan, J., Cheng, H., Edwards, R. L., Pons-Branchu, E. and Pierre, M.: A high-resolution fluid inclusion δ18O record from a stalagmite in SW France: modern calibration and comparison with multiple proxies, Quaternary Science Reviews, 110, 152–165, doi:10.1016/j.quascirev.2014.12.021, 2015.

Leuschner, D. C. and Sirocko, F.: The low-latitude monsoon climate during Dansgaard-Oeschger cycles and Heinrich Events, Quaternary Science Reviews, 19(1–5), 243–254, 2000.

Leuschner, D. C. and Sirocko, F.: Orbital insolation forcing of the Indian Monsoon - a motor for global climate changes?, Palaeogeography Palaeoclimatology Palaeoecology, 197(1–2), 83–95, 2003.

Liu, D., Wang, Y., Cheng, H., Lawrence Edwards, R., Kong, X., Wang, X., Hardt, B., Wu, J., Chen, S., Jiang, X., He, Y., Dong, J. and Zhao, K.: Sub-millennial variability of Asian monsoon intensity during the early MIS 3 and its analogue to the ice age terminations, Quaternary Science Reviews, 29(9), 1107–1115, doi:10.1016/j.quascirev.2010.01.008, 2010.

Lu, H.-Y., Wu, N.-Q., Liu, K.-B., Jiang, H. and Liu, T.-S.: Phytoliths as quantitative indicators for the reconstruction of past environmental conditions in China II: palaeoenvironmental reconstruction in the Loess Plateau, Quaternary Science Reviews, 26(5), 759–772, doi:https://doi.org/10.1016/j.quascirev.2006.10.006, 2007.

Martrat, B., Grimalt, J. O., Shackleton, N. J., Abreu, L. de, Hutterli, M. A. and Stocker, T. F.: Four Climate Cycles of Recurring Deep and Surface Water Destabilizations on the Iberian Margin, Science, 317(5837), 502–507, doi:10.1126/science.1139994, 2007.

Mingram, J., Stebich, M., Schettler, G., Hu, Y., Rioual, P., Nowaczyk, N., Dulski, P., You, H., Opitz, S., Liu, Q. and Liu, J.: Millennial-scale East Asian monsoon variability of the last glacial deduced from annually laminated sediments from Lake Sihailongwan, N.E. China, Quaternary Science Reviews, 201, 57–76, doi:10.1016/j.quascirev.2018.09.023, 2018.

Mulitza, S., Prange, M., Stuut, J.-B., Zabel, M., Dobeneck, T. von, Itambi, A. C., Nizou, J., Schulz, M. and Wefer, G.: Sahel megadroughts triggered by glacial slowdowns of Atlantic meridional overturning, Paleoceanography, 23(4), doi:10.1029/2008PA001637, 2008.

NOAA-NCDC weather service: NOAA-NCDC weather service, [online] Available from: https://www.ncdc.noaa.gov/ (Accessed 15 August 2018), 2018.

North Greenland Ice Core Project Members, Andersen, K. K., Azuma, N., Barnola, J.-M., Bigler, M., Biscaye, P., Caillon, N., Chappellaz, J., Clausen, H. B., Dahl-Jensen, D., Fischer, H., Flückiger, J., Fritzsche, D., Fujii, Y., Goto-Azuma, K., Grønvold, K., Gundestrup, N. S., Hansson, M., Huber, C., Hvidberg, C. S., Johnsen, S. J., Jonsell, U., Jouzel, J., Kipfstuhl, S., Landais, A., Leuenberger, M., Lorrain, R., Masson-Delmotte, V., Miller, H., Motoyama, H., Narita, H., Popp, T., Rasmussen, S. O., Raynaud, D., Rothlisberger, R., Ruth, U., Samyn, D., Schwander, J., Shoji, H., Siggard-Andersen, M.-L., Steffensen, J. P., Stocker, T., Sveinbjörnsdóttir, A. E., Svensson, A., Takata, M., Tison, J.-L., Thorsteinsson, T., Watanabe, O., Wilhelms, F. and White, J. W. C.: High-resolution record of Northern Hemisphere climate extending into the last interglacial period, Nature, 431(7005), 147–151, doi:10.1038/nature02805, 2004.

Reille, M. and de Beaulieu, J. L.: History of the Würm and Holocene vegetation in western velay (Massif Central, France): A comparison of pollen analysis from three corings at Lac du Bouchet, Review of Palaeobotany and Palynology, 54(3), 233–248, doi:10.1016/0034-6667(88)90016-4, 1988.

Reille, M. and de Beaulieu, J. L.: Pollen analysis of a long upper Pleistocene continental sequence in a Velay maar (Massif Central, France), Palaeogeography, Palaeoclimatology, Palaeoecology, 80(1), 35–48, doi:10.1016/0031-0182(90)90032-3, 1990.

Roucoux, K. H., de Abreu, L., Shackleton, N. J. and Tzedakis, P. C.: The response of NW Iberian vegetation to North Atlantic climate oscillations during the last 65kyr, Quaternary Science Reviews, 24(14), 1637–1653, doi:10.1016/j.quascirev.2004.08.022, 2005.

Ruth, U., Bigler, M., Röthlisberger, R., Siggaard-Andersen, M.-L., Kipfstuhl, S., Goto-Azuma, K., Hansson, M. E., Johnsen, S. J., Lu, H. and Steffensen, J. P.: Ice core evidence for a very tight link between North Atlantic and east Asian glacial climate, Geophysical Research Letters, 34(3), doi:10.1029/2006GL027876, 2007.

Schettler, G., Liu, Q., Mingram, J., Stebich, M. and Dulski, P.: East-Asian monsoon variability between 15 000 and 2000 cal. yr BP recorded in varved sediments of Lake Sihailongwan (northeastern China, Long Gang volcanic field), The Holocene, 16(8), 1043–1057, doi:10.1177/0959683606069388, 2006.

Schulz, H., von Rad, U., Erlenkeuser, H. and von Rad, U.: Correlation between Arabian Sea and Greenland climate oscillations of the past 110,000 years, Nature, 393(6680), 54–57, doi:10.1038/31750, 1998.

Sirocko, F., Garbe-Schönberg, D., McIntyre, A. and Molfino, B.: Teleconnections between the subtropical monsoon and high latitude climates during the last deglaciation, Science, 272, 526–529, 1996.

Sirocko, F., Knapp, H., Dreher, F., Förster, M. W., Albert, J., Brunck, H., Veres, D., Dietrich, S., Zech, M., Hambach, U., Röhner, M., Rudert, S., Schwibus, K., Adams, C. and Sigl, P.: The ELSA-Vegetation-Stack: Reconstruction of Landscape Evolution Zones (LEZ) from laminated Eifel maar sediments of the last 60,000years, Global and Planetary Change, 142, 108–135, doi:10.1016/j.gloplacha.2016.03.005, 2016.

Stebich, M., Rehfeld, K., Schlütz, F., Tarasov, P. E., Liu, J. and Mingram, J.: Holocene vegetation and climate dynamics of NE China based on the pollen record from Sihailongwan Maar Lake, Quaternary Science Reviews, 124, 275–289, doi:https://doi.org/10.1016/j.quascirev.2015.07.021, 2015.

Sun, Y., Wang, X., Liu, Q. and Clemens, S. C.: Impacts of post-depositional processes on rapid monsoon signals recorded by the last glacial loess deposits of northern China, Earth and Planetary Science Letters, 289(1–2), 171–179, doi:10.1016/j.epsl.2009.10.038, 2010.

Ünal-İmer, E., Shulmeister, J., Zhao, J.-X., Tonguç Uysal, I., Feng, Y.-X., Duc Nguyen, A. and Yüce, G.: An 80 kyr-long continuous speleothem record from Dim Cave, SW Turkey with paleoclimatic implications for the Eastern Mediterranean, Scientific Reports, 5(1), doi:10.1038/srep13560, 2015.

Wagner, J. D. M., Cole, J. E., Beck, J. W., Patchett, P. J., Henderson, G. M. and Barnett, H. R.: Moisture variability in the southwestern United States linked to abrupt glacial climate change, Nature Geoscience, 3(2), 110–113, doi:10.1038/ngeo707, 2010.

Wainer, K., Genty, D., Blamart, D., Hoffmann, D. and Couchoud, I.: A new stage 3 millennial climatic variability record from a SW France speleothem, Palaeogeography, Palaeoclimatology, Palaeoecology, 271(1–2), 130–139, doi:10.1016/j.palaeo.2008.10.009, 2009.

Wang, Y. J., Cheng, H., Edwards, R. L., An, Z. S., Wu, J. Y., Shen, C.-C. and Dorale, J. A.: A High-Resolution Absolute-Dated Late Pleistocene Monsoon Record from Hulu Cave, China, Science, 294(5550), 2345, doi:10.1126/science.1064618, 2001.

Wassenburg, J. A., Immenhauser, A., Richter, D. K., Jochum, K. P., Fietzke, J., Deininger, M., Goos, M., Scholz, D. and Sabaoui, A.: Climate and cave control on Pleistocene/Holocene calcite-to-aragonite transitions in speleothems from Morocco: Elemental and isotopic evidence, Geochimica et Cosmochimica Acta, 92, 23–47, doi:10.1016/j.gca.2012.06.002, 2012.

Wassenburg, J. A., Dietrich, S., Fietzke, J., Fohlmeister, J., Jochum, K. P., Scholz, D., Richter, D. K., Sabaoui, A., Spötl, C., Lohmann, G., Andreae, M. O. and Immenhauser, A.: Reorganization of the North Atlantic Oscillation during early Holocene deglaciation, Nature Geoscience, 9(8), 602–605, doi:10.1038/ngeo2767, 2016.

Watts, W. A.: A long pollen record from Laghi di Monticchio, southern Italy: a preiminary account, Journal of the Geological Society, 142(3), 491–499, doi:10.1144/gsjgs.142.3.0491, 1985.